Electronic Supplementary Information

Two-dimensional XC_6-enes (X=Ge, Sn, Pb) with moderate band gaps, biaxial negative Poisson's ratios, and high carrier mobilities

Hongxia Bu [a, *], Xiaobiao Liu [b], Huimin Yuan [a], Xiaojuan Yuan [a], Jingfen Zhao [a], Mingwen Zhao [c, *]

[a] *College of Physics and Electronic Engineering, Qilu Normal University, Jinan, Shandong 250200, China*

[b] *College of Science, Henan Agricultural University, Zhengzhou, Henan 450002, China*

[c] *School of Physics & State Key Laboratory of Crystal Materials, Shandong University, Jinan, Shandong 250100, China*

Corresponding authors. E-mails: buhx666@163.com (Hognxia Bu), zmw@sdu.edu.cn (Mingwen Zhao)

Table S1 The calculated lattice constant (Å) and Wyckoff positions of C atoms in XC_6-enes (X=Ge, Sn, Pb). X atom occupied the 4b (0.250, 0.500, 0.500) Wyckoff position in XC_6-enes.

	a(Å)	b(Å)	Wyckoff positions
GeC_6-ene	10.710	7.922	8m (0.000, 0.418, 0.516) 16o (0.116, 0.338,0.528)
SnC_6-ene	11.407	8.213	8m (0.000, 0.417, 0.513) 16o (0.17, 0.335, 0.525)
PbC_6-ene	11.720	8.313	8m (0.000, 0.417, 0.513) 16o (0.103, 0.333, 0.525)

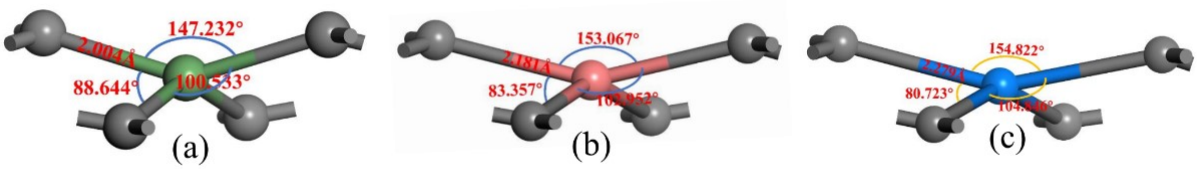

Fig.S1 The structure parameters of the (a) $[GeC_4]$, (b) $[SnC_4]$, and (c) $[PbC_4]$ units in the XC_6-enes (X=Ge, Sn, Pb).

Table S2 The calculated buckled height Δ (Å); bond length of B1, B2, B3 (labeled in Fig. 1(a)), and X-C (Å) as labeled in Fig. 1(c); non-bonding distances between C atoms (Å) (labeled as d1, d2, and d3 in Fig. 1(c)); cohesive energy, Ecoh (eV/atom) and formation energy (E_{form}) of XC_6-enes (X=Ge, Sn, Pb). For comparison, the corresponding values of graphene, g-GeC and g-SnC are also presented.

	Δ (Å)	B1 (Å)	B2 (Å)	B3 (Å)	X-C (Å)	d1 (Å)	d2 (Å)	d3 (Å)	E_{coh}（eV/atom）	E_{form}（eV/atom）
GeC_6-ene	1.131	1.398	1.416	1.448	2.004	2.801	3.083	3.846	-7.963	1.257
SnC_6-ene	1.016	1.394	1.418	1.466	2.178	2.895	3.408	4.237	-7.817	1.268
PbC_6-ene	0.993	1.387	1.416	1.472	2.262	2.952	3.612	4.448	-7.582	0.848
graphene	0	1.424/1.42[11]	--	--	--	--	--	--	-9.212	0
g-GeC	0	--	--	--	1.875/1.86[11]	--	--	--	-5.929	3.312
g-SnC	0	--	--	--	2.072/2.05[11]	--	--	--	-5.296	3.477

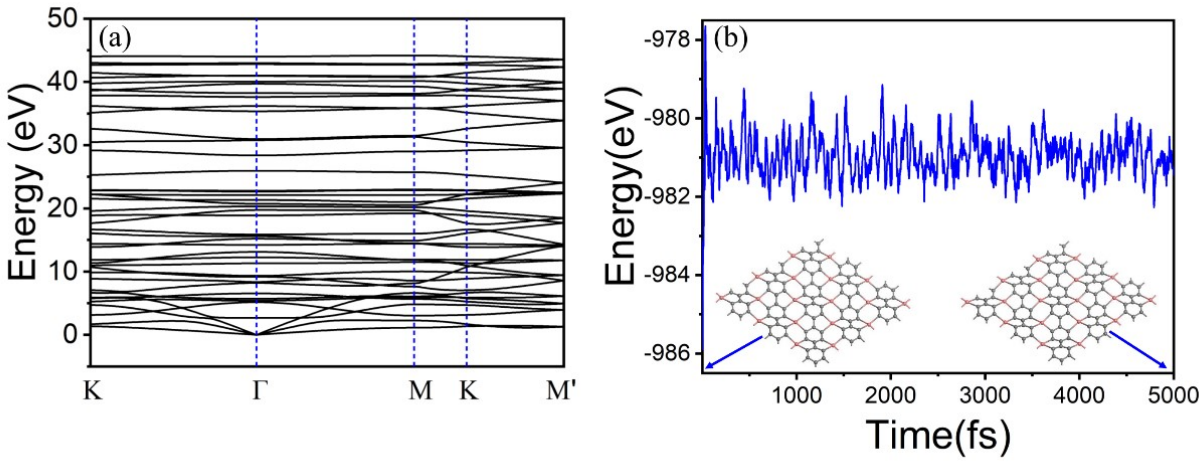

Fig. S2 (a) phonon spectrum of SnC_6-ene along the high symmetry direction of the first Brillouin zone as shown in Fig. 1(d), and (b) the total energy fluctuations with respect to the simulation time at 300 K, accompanied with the atomic structure snapshots.

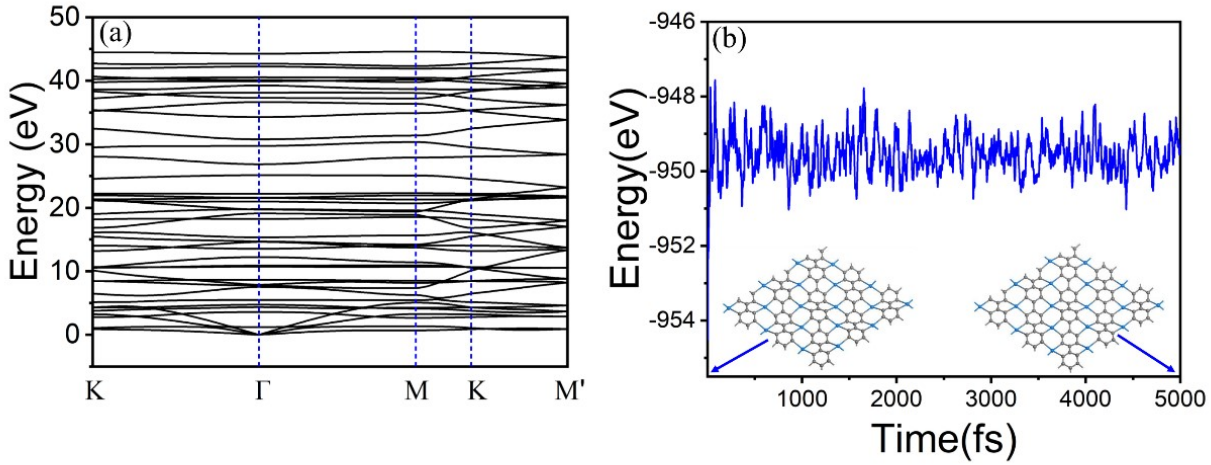

Fig. S3 (a) phonon spectrum of PbC_6-ene along the high symmetry direction of the first Brillouin zone as shown in Fig. 1(d), and (b) the total energy fluctuations with respect to the simulation time at 300 K, accompanied with the atomic structure snapshots.

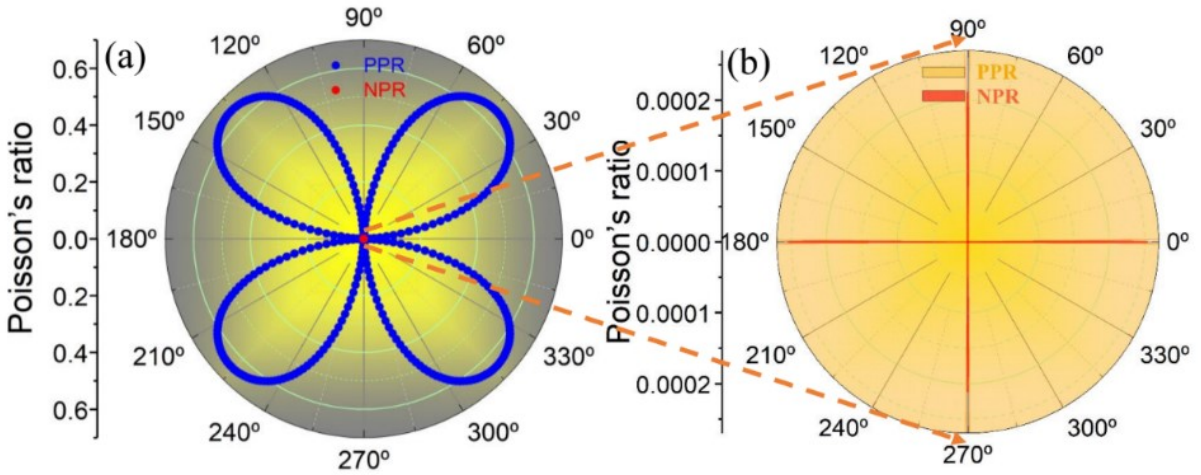

Fig. S4 Polar diagrams of (a) Poisson's ratio ν(θ) and (b) the Poisson's ratio ν(θ) region nearby the origin of the SnC_6-ene. Here θ=0° and θ=90° stand for the *x*-axis and *y*-axis as Fig.1, respectively.

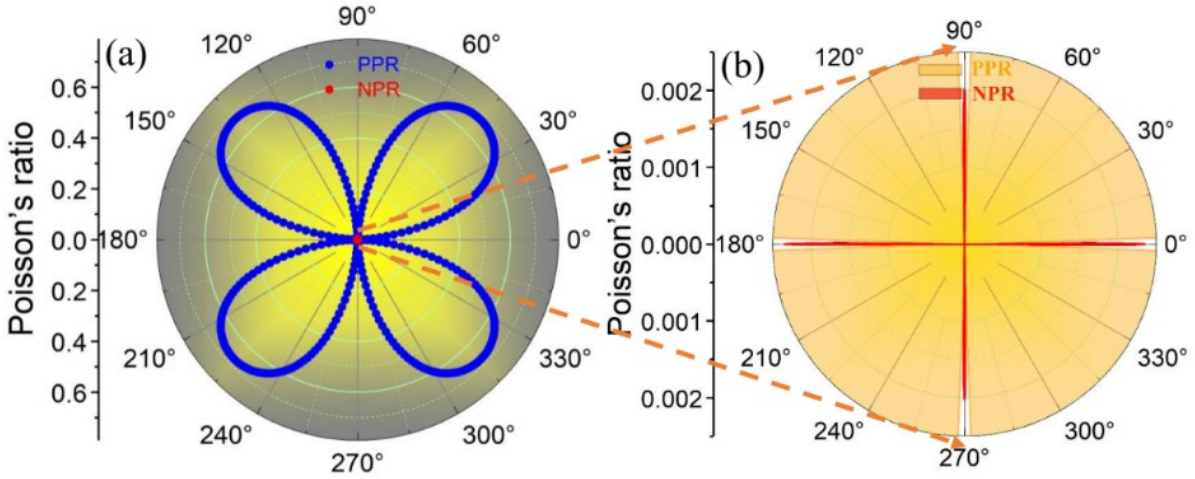

Fig. S5 Polar diagrams of (a) Poisson's ratio ν(θ) and (b) the Poisson's ratio ν(θ) region nearby the origin of the PbC_6-ene. Here θ=0° and θ=90° stand for the *x*-axis and *y*-axis as Fig.1 (a), respectively.

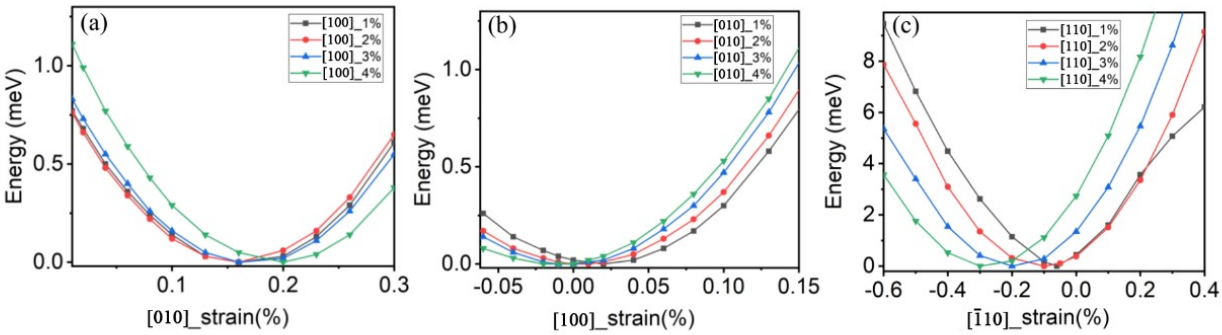

Fig. S6 Calculated strain energy with respect to the lateral response when the SnC_6-ene lattice endures a tensile strain in the (a) x-direction, (b) y-direction, and (c) diagonal-direction.

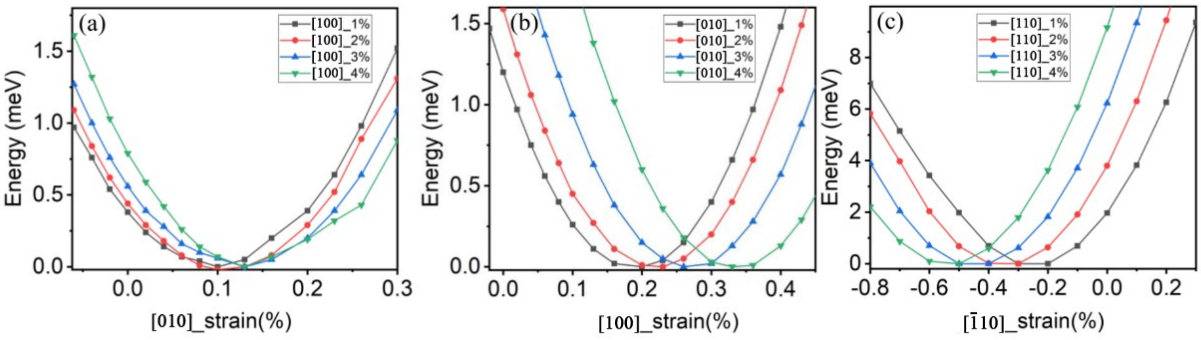

Fig. S7 Calculated strain energy with respect to the lateral response when the PbC_6-ene lattice endures a tensile strain in the (a) x-direction, (b) y-direction, and (c) diagonal-direction.

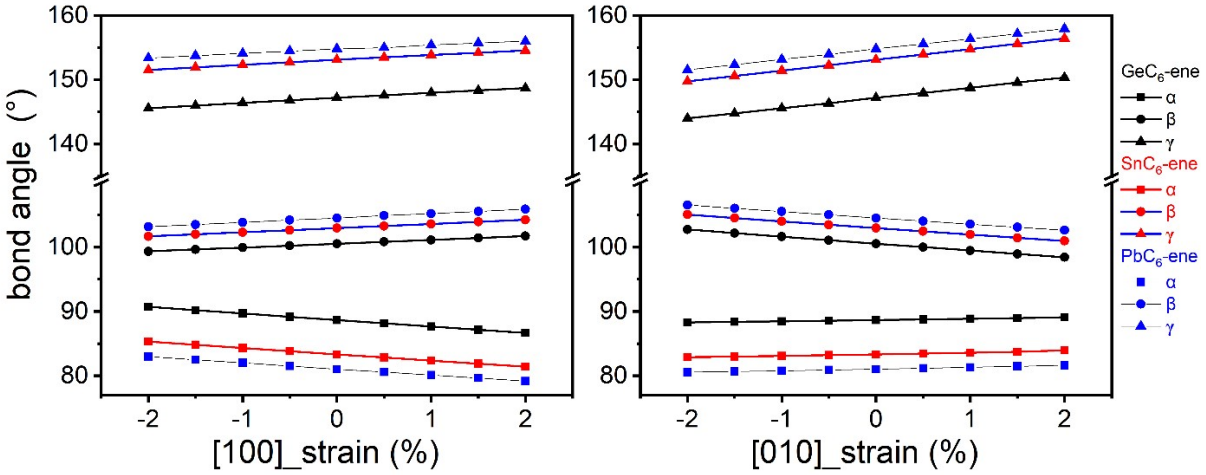

Fig. S8 Calculated bond angles (labeled in Fig. 1(c)) under the uniaxial strain.

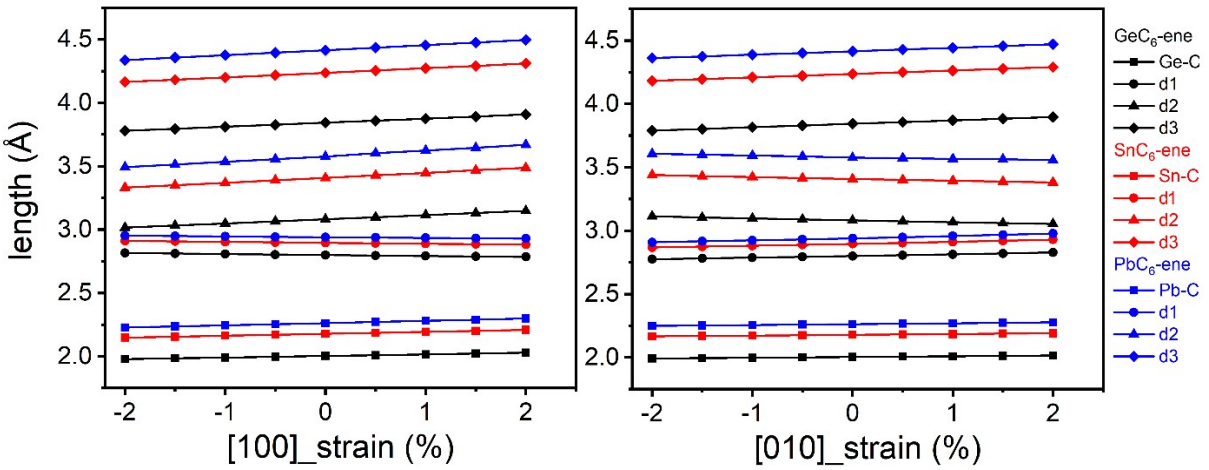

Fig. S9 Calculated X-C bond lengths, and the non-bonding distances d1, d2, and d3 (labeled in Fig. 1(a) and (c)) under the uniaxial strain.

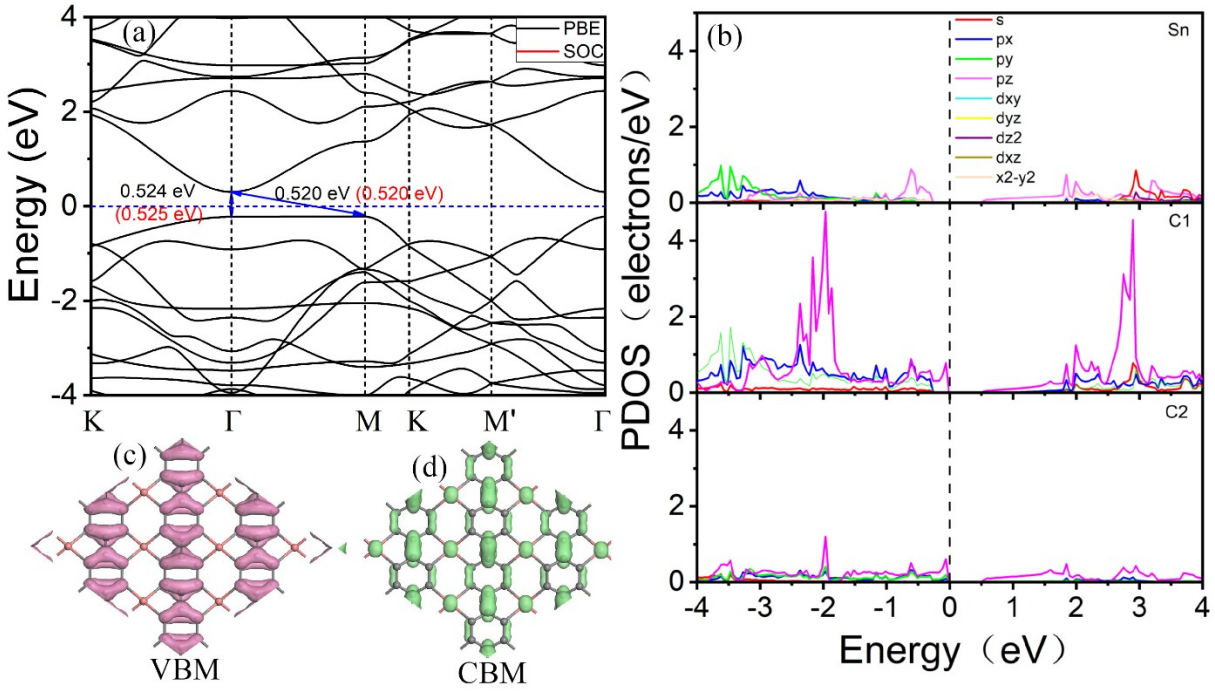

Fig. S10 (a) the band structures along the high symmetry directions in the first Brillouin zone, (b) the orbital-resolved electron density of states (PDOS) of SnC_6-ene projected onto different Sn and C atoms as labelled in Fig. 1 (a). The Fermi level was set to zero. Isosurfaces of the Kohn-Sham wavefunctions near Fermi surface of (c) VBM and (d) CBM.

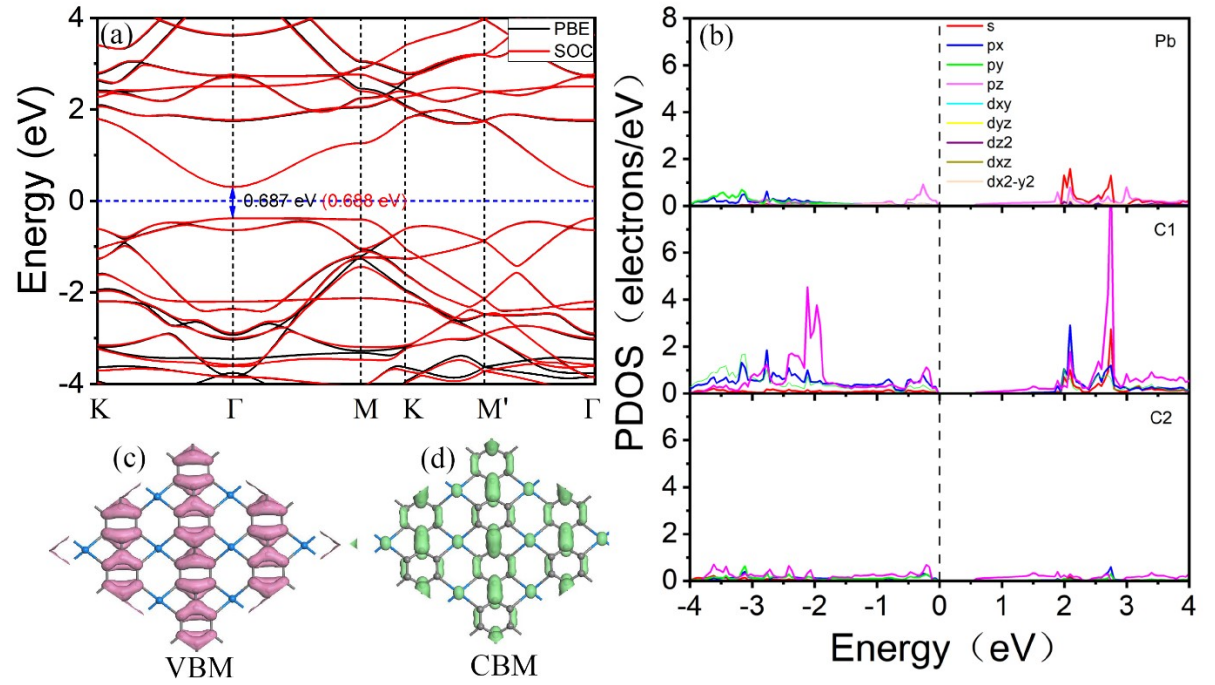

Fig. S11 (a) the band structures along the high symmetry directions in the first Brillouin zone, (b) the orbital-resolved electron density of states (PDOS) of PbC_6-ene projected onto different Pb and C atoms as labelled in Fig. 1 (a). The Fermi level was set to zero. Isosurfaces of the

Kohn-Sham wavefunctions near Fermi surface of (c) VBM and (d) CBM.

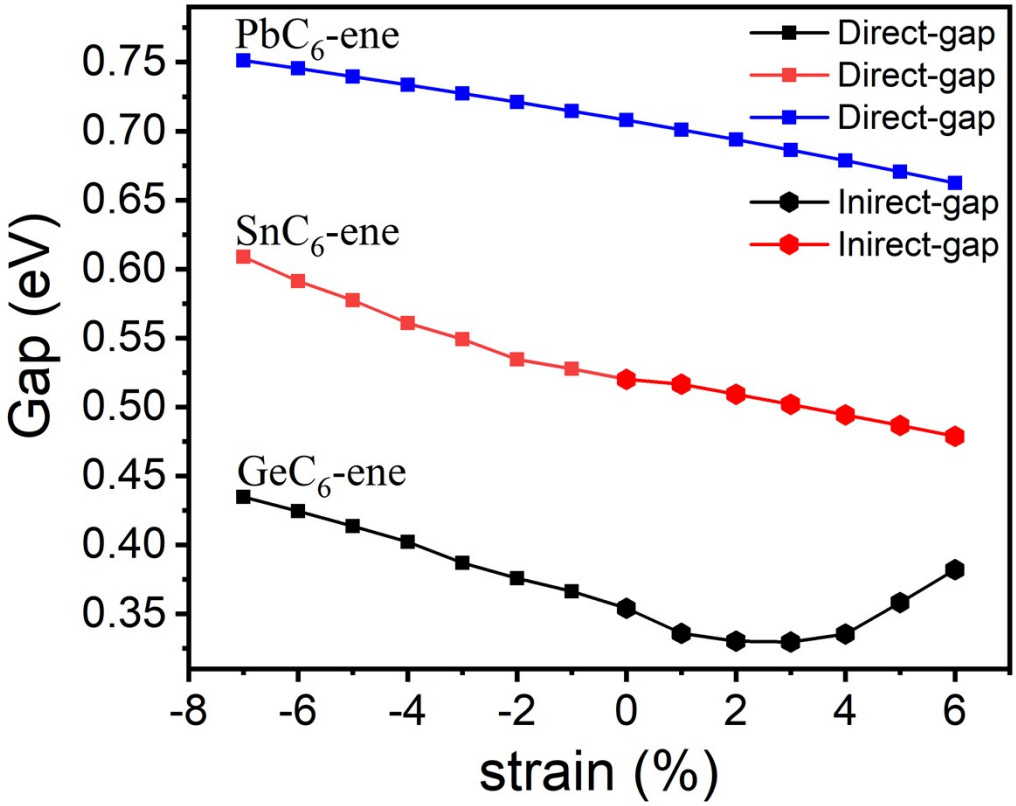

Fig. S12 Calculated band gaps under external strain for GeC_6-ene, SnC_6-ene, and PbC_6-ene.

References

[11] H. Şahin, S. Cahangirov, M. Topsakal, E. Bekaroglu, E. Akturk, R. T. Senger, et al, Monolayer honeycomb structures of group-IV elements and III-V binary compounds: First-principles calculations, Phys. Rev. B 80 (2009) 155453.